

## ONLINE DATA

### DETAILED METHODS

**Cell isolation and culture.** VSMCs were obtained from the aortas of male Sprague-Dawley rats (5 weeks old) by using an enzymatic dissociation method as described previously (9). VSMCs were cultured with DMEM containing 10% fetal bovine serum and 1% penicillin/streptomycin (Life Technologies, Carlsbad, CA). For all experiments, rat VSMCs from passages 3 to 6 were used. For the platelet study, mouse (C57BL/6, 6–8 weeks old) platelets were isolated using platelet-rich plasma (PRP) and the gel-filtration method as described in our previous studies (10). For the leukocyte study, mouse monocytes from blood were used. Mouse monocytes were isolated as described previously (11). In addition, human monocytic cell line, THP-1 cells from American Type Culture Collection (ATCC, Manassas, VA) were also used in some experiments. THP-1 cells were cultured in RPMI 1640 (Life Technologies, Carlsbad, CA) medium containing 10% fetal bovine serum and 1% penicillin/streptomycin. THP-1 cells were stimulated by 100 nmol/L phorbol-12-myristate-13-acetate (PMA, EMD Biosciences, San Diego, CA) for 24 hours to induce THP-1 macrophage.

**Isolation of blood microparticles.** Microparticles from serum were isolated by ultracentrifugation as described previously (4, 5). Briefly, the samples were filtered through a 0.22  $\mu\text{m}$  Millex-GS Filter Unit (Millipore, Billerica, MA), followed by ultracentrifugation at 130,000  $\times$  g for 2 h to pellet the microparticles. The pellet microparticles were resuspended in PBS to perform the experiments.

**RNA isolation, qRT-PCR and qRT-PCR-based absolute quantification.** RNAs from cultured cells, culture medium, serum, microparticles, rat carotid arteries, mouse carotid arteries and aortas, and human arteries were isolated with TRIzol (Life Technologies, Carlsbad, CA). For miRNA, cDNA was generated from 100 ng of total RNA using TaqMan MiRNA Reverse Transcription and TaqMan MiRNA assays (Life Technologies, Carlsbad, CA) (15-17). For other RNAs, cDNA was generated from 200 ng of total RNA using High-Capacity RNA-to-cDNA Kit (Life Technologies, Carlsbad, CA). qRT-PCR for both miRNA and mRNA were performed on cDNAs using TaqMan Fast Universal PCR Master Mix (2X), no AmpErase UNG (Life Technologies, Carlsbad, CA), according to the manufacturer's instructions. Amplification and detection of specific products were performed with a Life Technologies 480 ViiA 7 Detection System (Life Technologies, Carlsbad, CA). As an internal control, U6 was used for miRNA template normalization and GAPDH was used for other template normalizations. Fluorescent signals were normalized to an internal reference, and the threshold cycle (Ct) was set within

the exponential phase of the PCR. Relative gene expression was calculated by comparing cycle times for each target PCR. The target PCR Ct values were normalized by subtracting the U6 or GADPH Ct value, which provided the  $\Delta$ Ct value. Relative expression between treatments was then calculated using the following equation:  $\text{relative gene expression} = 2^{-(\Delta\text{Ct sample} - \Delta\text{Ct control})}$ . The absolute quantification of a miRNA was based on qRT-PCR and a standard curve using a series of concentrations of synthesized mature miRNA (4, 5) and was expressed as pmol/L, copies/cell or copies/15 pg tissue RNA.

**MiRNA expression profiles.** The profiles of miRNAs in serum, blood cells (platelets, leukocytes) and blood microparticles by stem-loop RT-PCR-based Rodent MicroRNA TaqMan low-density arrays (TLDA) (Applied Biosystems, Carlsbad, CA). Comprehensive coverage of rodent miRNA species in Sanger miRBase v15 was enabled across a two-card set of TaqMan Array Rodent MiRNA Cards (Card A v2.0 and Card B v3.0) according to the manufacturer's recommended protocol (Applied Biosystems, Carlsbad, CA). Human miRNA profiling was performed using human TaqMan low density array A (v2.0) according to the manufacturer's recommended protocol (Applied Biosystems, Carlsbad, CA).

**Oligonucleotide transfection and gene modulation in cultured VSMCs.** Oligonucleotide transfection was performed as described in our previous studies (5, 9). Briefly, cells were transfected using a transfection reagent (Qiagen, Valencia, CA) 24 hours after seeding into the wells. Transfection complexes were prepared according to the manufacturer's instructions. The expression of miR-223 was downregulated by its inhibitor (Anti-miR miRNA Inhibitor, Life Technologies, Carlsbad, CA), and was upregulated via its mimics (mirVana miRNA mimic, Life Technologies, Carlsbad, CA) (1-30 nM). The transfection medium was replaced 4 hours posttransfection by the regular culture medium. Vehicle and scramble controls (Integrated DNA Technologies, Coralville, IA) were applied.

**Monitoring the secretion of miR-223 by leukocytes and its ability to enter into VSMCs.** In this experiment, culture medium was collected before and after 12 hours of THP-1 macrophages culture. Then, the medium was filtered by 0.22  $\mu$ m Millex-GS Filter Unit (Millipore, Billerica, MA) to remove cells. The levels of miR-223 in collected medium were determined by qRT-PCR. In addition, the collected medium after 12 hours of THP-1 macrophages culture was added to the cultured medium of VSMCs. After 12 hours, levels of miR-223 in VSMCs were determined by qRT-PCR.

**Monitoring the secretion of fluorescence-marked miR-223 by leukocytes and its ability to enter into VSMCs.** In this experiment, the 0.4 $\mu$ m Boyden chambers (Corning, Corning, NY) co-

culture system was applied. THP-1 macrophages were prepared in the upper chamber and then transfected with Cy3-marked miR-223 (Ribobio, China). THP-1 macrophages without Cy3-marked miR-223 were used as controls. After transfection, the THP-1 macrophages were washed with PBS for 3 times to remove extracellular Cy3-marked miR-223. VSMCs were added into the lower chamber. Thus, THP-1 macrophages did not contact with VSMCs directly. However, the culture medium could be freely movement between the two chambers. Secretion of Cy3-marked miR-223 and its ability to enter into VSMCs were monitored by fluorescence microscope.

**miR-223 inhibition in mice in vivo.** miR-223 expression in vivo in mice was knocked down by the in vivo LNA™ microRNA Inhibitor for miR-223 (LN-anti-miR-223) from Exiqon (30mg/kg, ip, biweekly). A scramble control (Integrated DNA Technologies, Coralville, IA) was applied in this study.

**Western blot analysis.** Proteins were isolated from cultured VSMCs, and the protein levels were determined by Western blot analysis. Briefly, equal amounts of protein were subjected to SDS-PAGE. Standard Western blot analysis was conducted using antibodies for IGF-1R (1:1000 dilution; Cell Signaling Technology, Danvers, MA), Akt (1:1000 dilution; Cell Signaling Technology, Danvers, MA), phospho-Akt (p-Akt, ser473, 1:1000 dilution; Cell Signaling Technology, Danvers, MA). GAPDH antibody (1:2000 dilution; Cell Signaling Technology, Danvers, MA) was used as a loading control.

**Luciferase assay.** A construct in which a fragment of the 3'-UTR of insulin-like growth factor 1 receptor (IGF-1R) mRNA containing the putative miR-223 binding sequences was cloned into a firefly luciferase reporter and transfected into HEK 293 cells (0.2 µg/ml). The cells were co-transfected with vehicle (vehicle), an empty plasmid (pDNR-CMV, 0.2 µg/ml), a plasmid expressing miR-223 (pmiR-223, 0.2 µg/ml). In addition, the constructs with mutated fragment of the 3'-UTR of IGF-1R mRNA without the putative miR-223 binding sequences (0.2 µg/ml) were used as mutated controls. Relative luciferase activity was measured on a scintillation counter by using a dual luciferase reporter system.

**Cell proliferation, migration and apoptosis.** VSMC proliferation was induced by platelet-derived growth factor (PDGF) (20 ng/ml) and was determined by MTT (Roche, Mannheim, Germany) assay and 5-ethynyl-2'-deoxyuridine (EdU, Ribobio, China) assay (12). For MTT assay, cells were incubated with MTT labeling reagent in a humidified atmosphere for 4 hours (37°C, 5% CO<sub>2</sub>). Then, solubilization solution was added and incubated in a humidified atmosphere overnight (37°C, 5% CO<sub>2</sub>). Absorbance was measured at 580 nm and 680 nm. For

EdU assay, the cells were incubated with EdU (50  $\mu$ M) for 2 h and then fixed with 4% paraformaldehyde for 30 min. The cells were then treated with 100  $\mu$ L of Apollo reaction cocktail for 30 min, followed by 100  $\mu$ L of 1% Hoechst 33342 for 30 min for nuclear staining. Finally, the proliferative cells were detected under a fluorescence microscope. VSMC migration was determined by a modified Boyden chamber assay (12). For the modified Boyden chamber assay, the upper inserts (24-well insert, 8 $\mu$ m pore size, BD Biosciences, Franklin Lakes, NJ) containing VSMCs ( $1 \times 10^5$  cells) resuspended in DMEM were placed in the bottom of 24-well chamber containing DMEM with 10% fetal bovine serum. After incubation for 6 h at 37°C, the cells passing through the membrane onto the lower side of the chamber were fixed with 4% formaldehyde and stained with 0.1% crystal violet for 10 min. The migrated cells were then counted in nine random 10  $\times$  high-power microscope fields. VSMC apoptosis in cultured cells was measured by TUNEL analysis after 48 h in serum-free culture as described (12). The VSMCs cultured on coverslips in 24-well plates were fixed in 4% paraformaldehyde. TUNEL staining was done using the In Situ Cell Death Detection Kit (Roche, Mannheim, Germany) according to the manufacturer's protocol. The number of TUNEL-positive cells was counted under a fluorescence microscope. Apoptotic cells were quantified by counting the percentage of TUNEL-positive cells against total nucleated cells stained by DAPI.

**Leukocyte or platelet depletion.** The well-established leukocyte depletion and platelet depletion models in male wild type C57BL/6 mice (3 months old) were used as described previously (13, 14). Briefly, the mice will be injected with control antibodies, Vinblastine (2.5 mg/kg, ip; Sigma-Aldrich) (for Neutrophil depletion) or rabbit anti-mouse thrombocyte serum (50  $\mu$ L i.p.) (Accurate Chemical Corp). The successful depletion was monitored by blood leukocyte and platelet quantification.

**Mouse atherosclerosis model.** Atherosclerosis was induced in the aortas of ApoE-knockout male mice on a C57BL/6 background (Jackson Laboratories) by a Western diet containing 21% fat, 0.15% cholesterol, and 19.5% casein (TestDiet, Richmond, IN) for 12 weeks as described previously (13). The mice were purchased at 5-week-old. At the beginning of 6-week-old, the animals were divided into the following groups: 1) ApoE<sup>-/-</sup> mice fed with the Western diet and treated with miR-223 inhibitor LN-anti-miR-223 (30mg/kg, ip. biweekly); 2) ApoE<sup>-/-</sup> mice fed with the Western diet and treated with a scramble control (30mg/kg, ip. biweekly).

**Measurement of atherosclerosis in mice.** The animals were euthanized with over dose of pentobarbital (200mg/kg, ip). Atherosclerotic lesions were measured by oil red O staining using en face preparation of whole aortas as shown in our previous publications (13). For the oil red O

staining, the aortas dissected from the ascending aorta to the iliac bifurcation were freed of adherent connective tissues and then cut longitudinally. The aortas were fixed in 4% paraformaldehyde and stained with oil-red O (Sigma-Aldrich, ST. Louis, MO) to visualize the atherosclerotic plaque area (fatty streaks) (13). The lesion area was calculated using Image-Pro Plus 6.0 software (Media Cybernetics, Rockville, MD).

**Rat carotid artery balloon injury model.** Carotid artery balloon injury was induced in male Sprague-Dawley rats (230 to 300 g) as described in our previous studies (9). Rats were anesthetized with ketamine (80 mg/kg)/xylazine (5 mg/kg). Under a dissecting microscope, the right common carotid artery was exposed through a midline cervical incision. A 2F Fogarty catheter (Edwards Lifesciences, Irvine, CA) was introduced via an arteriotomy in the external carotid artery, and then the catheter was advanced to the proximal edge of the omohyoid muscle. To produce carotid artery injury, we inflated the balloon with saline and withdrew it 3 times from just under the proximal edge of the omohyoid muscle to the carotid bifurcation. After balloon injury, the external carotid artery was then permanently ligated with a 6-0 silk suture, and blood flow in the common carotid artery was restored.

**miR-223 knockout mice.** miR-223 knockout mice were produced and provided by The Jackson Laboratory. In this strain with C57BL/6 background, the allele replaces the entire coding region of the miR-223 gene with a frt-flanked neomycin resistance cassette, abolishing gene function. We verified it by qRT-PCR showing that there was no expression of miR-223 in these knockout mice.

**Mouse carotid artery ligation injury model.** Right carotid artery ligation injury was induced in male wild type C57BL/6 mice (3 months old) and in age matched miR-223 knockout mice as described in our previous study (15). The common carotid artery was ligated permanently with a 7-0 silk suture just proximal to its bifurcation. The mice were sacrificed at 4 weeks following the vascular injury. The right atria of the animals were dissected, and a 24-gauge catheter connected to the perfusion system was inserted in left ventricle. All the animals were perfusion-fixed for 5 min with 10% formalin at physiological pressure. The right common carotid arteries were removed and the proximal 1mm and distal 3mm regions were discarded. The remaining portion (~5mm) of the artery was embedded in paraffin, and serial sections (5  $\mu$ m thick) were made for the morphometric analysis.

**Morphometric analysis for neointimal lesion formation in carotid arteries from mice.** Morphometric analysis via computerized image analysis system (NIS Elements BR 3.0) was performed in sections stained with H-E staining as described (9,15). In brief, 6 sections (5  $\mu$ m

thick) sectioned at equally spaced intervals of mouse carotid arteries were used. The intimal-to-medial area ratio of each section was calculated. The average intimal-to-medial area ratio of the 6 sections was used as the intimal-to-medial area ratio of each animal. All animal protocols were approved by the Institutional Animal Care and Use Committee at Rush University and were consistent with the Guide for the Care and Use of Laboratory Animals (updated (2011) version of the NIH guidelines).

**Human serum and vessel samples.** This study was approved by the research ethics committee of the First Affiliated Hospital of Sun Yat-sen University and was performed conform the declaration of Helsinki. Human serum samples were from health subjects (n=8) and from patients with atherosclerosis (n=8). All data were de-identified before being provided to the investigators. The atherosclerotic arteries (n=6) were obtained from patients with arteriosclerosis obliterans who underwent lower limb amputation and the normal lower limb artery samples (n=6) were acquired from donors without arteriosclerosis obliterans with the informed consent of all subjects. Note: the totally blocked arteries were avoid due to the 100% stenosis, in which the segment cannot contact with circulating serum.

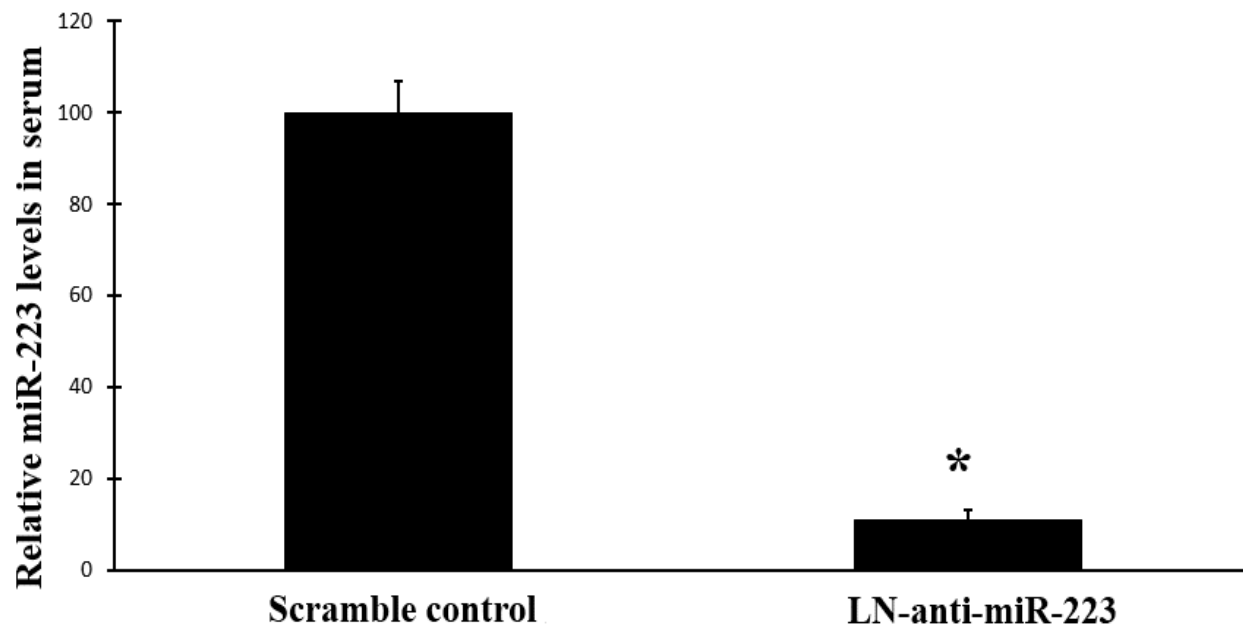
**Statistics.** All data are presented as mean±standard error. For relative gene expression, the mean value of the vehicle control group is defined as 100% or 1. Two-tailed unpaired Student *t* tests and ANOVAs were used for statistical evaluation of the data. SPSS 17.0 was used for data analysis. A  $P<0.05$  was considered significant.

**Table 1. The list of top 5 most abundant miRNAs in serum microparticles, platelets and leukocytes**

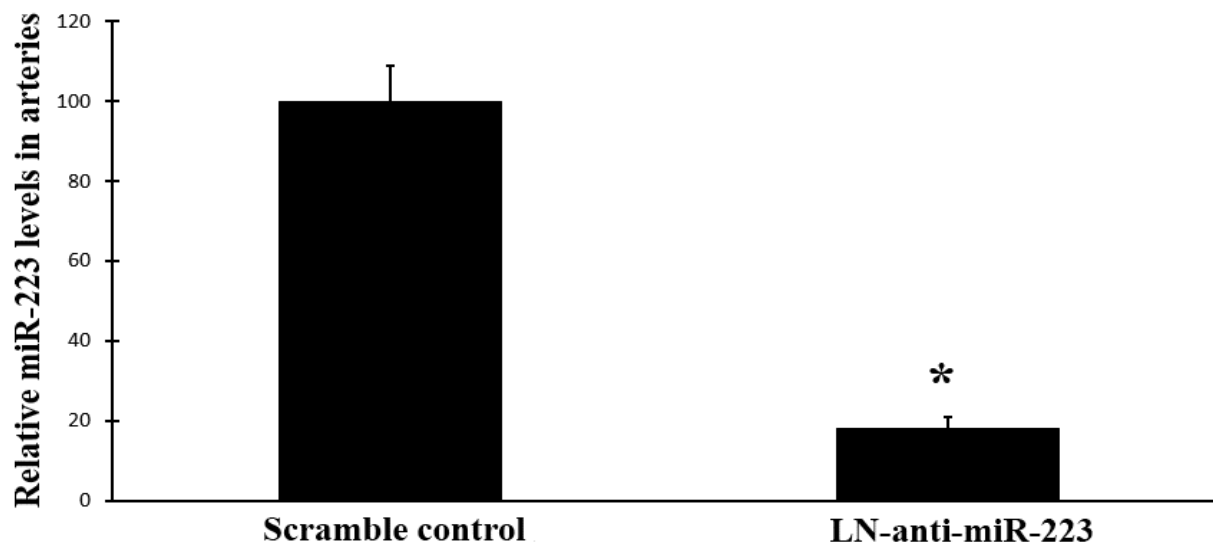
| Rank #         | 1       | 2        | 3       | 4        | 5       |
|----------------|---------|----------|---------|----------|---------|
| Microparticles | miR-223 | miR-146a | miR-16  | miR-484  | miR-451 |
| Platelets      | miR-223 | miR-16   | miR-126 | miR-451  | miR-19B |
| Leukocytes     | miR-223 | miR-150  | miR-16  | miR-146b | miR-451 |

**Table 2. The list of top 5 most abundant miRNAs in serum from human, mouse and rat**

| Rank # | 1       | 2       | 3       | 4       | 5        |
|--------|---------|---------|---------|---------|----------|
| Human  | miR-223 | miR-451 | miR-92a | miR-19b | miR-1974 |
| Mouse  | miR-223 | miR-451 | miR-92a | miR-19b | miR-24   |
| Rat    | miR-223 | miR-451 | miR-92a | miR-19b | miR-16   |

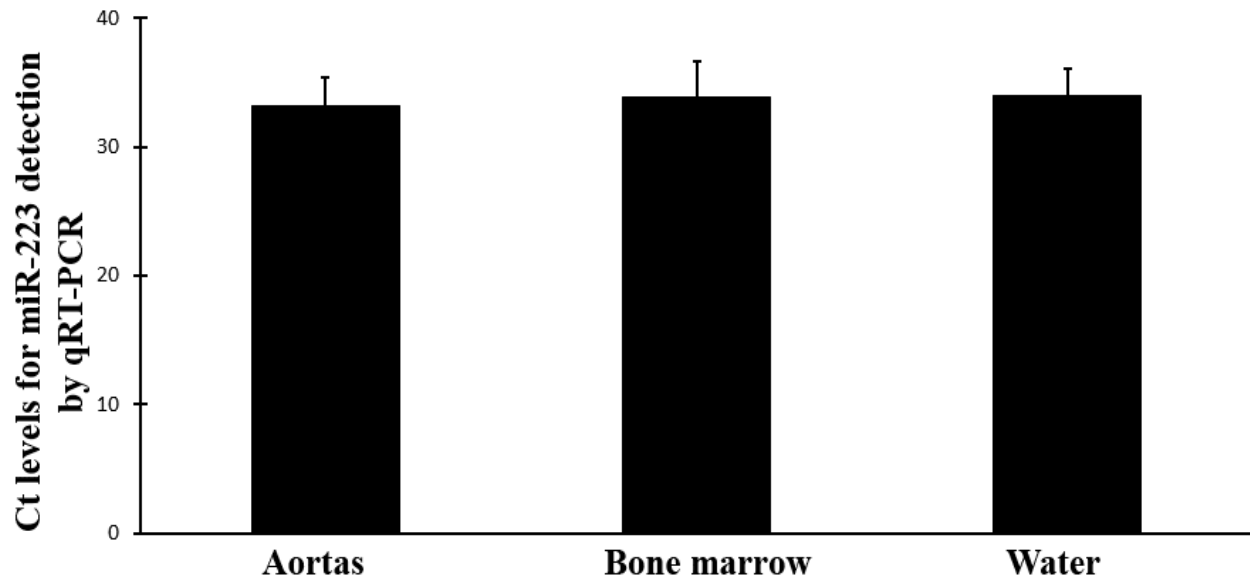


Online Fig. 1. The serum levels of miR-223 in mice were successfully knocked down by LN-anti-miR-223 (30mg/kg, iv. via tail vein, biweekly). Note: n=6; \*p<0.05 compared with control groups.



Online Fig. 2. The vascular levels of miR-223 in mice were successfully knocked down by LN-anti-miR-223 (30mg/kg, iv. via tail vein, biweekly). Note: n=6; \*p<0.05 compared with control groups.





Online Fig. 3. No miR-223 expression in miR-223 knockout mice. The aortas and bone marrow of miR-223 knockout mice were isolated (n=3) and miR-223 was determined by qRT-PCR. No miR-223 expression was found as the Ct was close to the level of negative control group (water).